

Catalytic and SERS activities of WO₃-based nanowires: The effect of oxygen vacancy, silver nanoparticle doping, and the type of organic dyes

Oguzhan Ustun^a, Asli Yilmaz^b, Mehmet Yilmaz^{a,c*}

^aDepartment of Nanoscience and Nanoengineering, Ataturk University, 25240 Erzurum, Turkey

^bDepartment of Molecular Biology and Genetics, Ataturk University, 25240 Erzurum, Turkey

^cDepartment of Chemical Engineering, Ataturk University, 25240 Erzurum, Turkey

*Correspondence: MY, nano.yilmaz@gmail.com

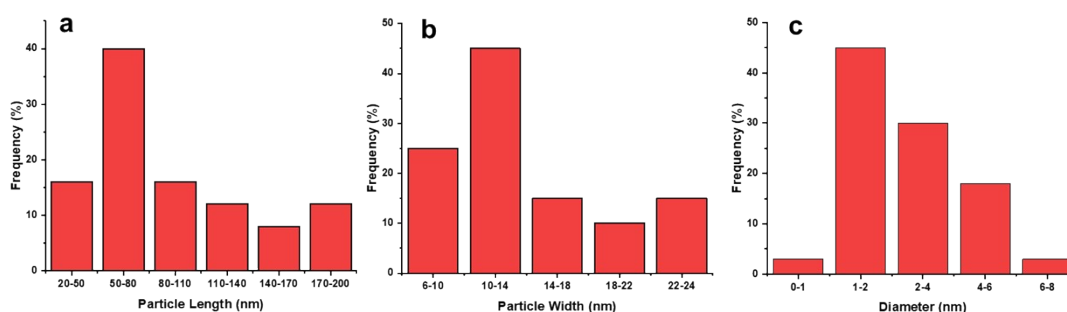
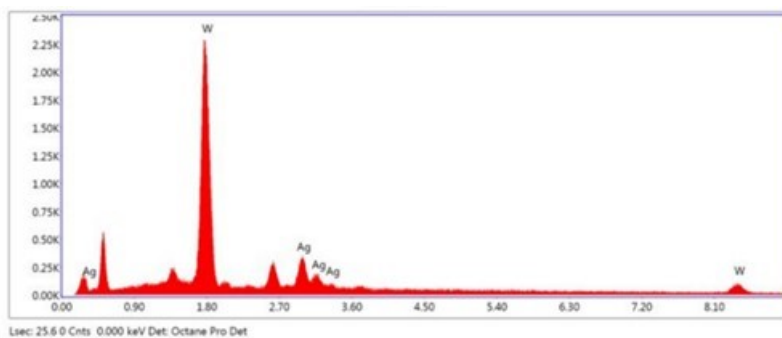


Figure S1. The particle length (a) and width (b) distribution for WO_{3-x} NPs and diameter of Ag nanostructures (c) for WO_{3-x}@Ag NPs.



Lsec: 25.60 Cnts 0.000 keV Det: Octane Pro Det

eZAF Smart Quant Results

Element	Weight %	Atomic %	Net Int.	Error %	Kratio	Z	R	A	F
WM	81.20	71.70	1,568.14	2.71	0.79	0.97	1.02	0.99	1.02
AgL	18.80	28.30	251.95	8.91	0.15	1.12	0.93	0.72	1

Figure S2. EDX spectra of $\text{WO}_{3-x}@Ag$ NPs.

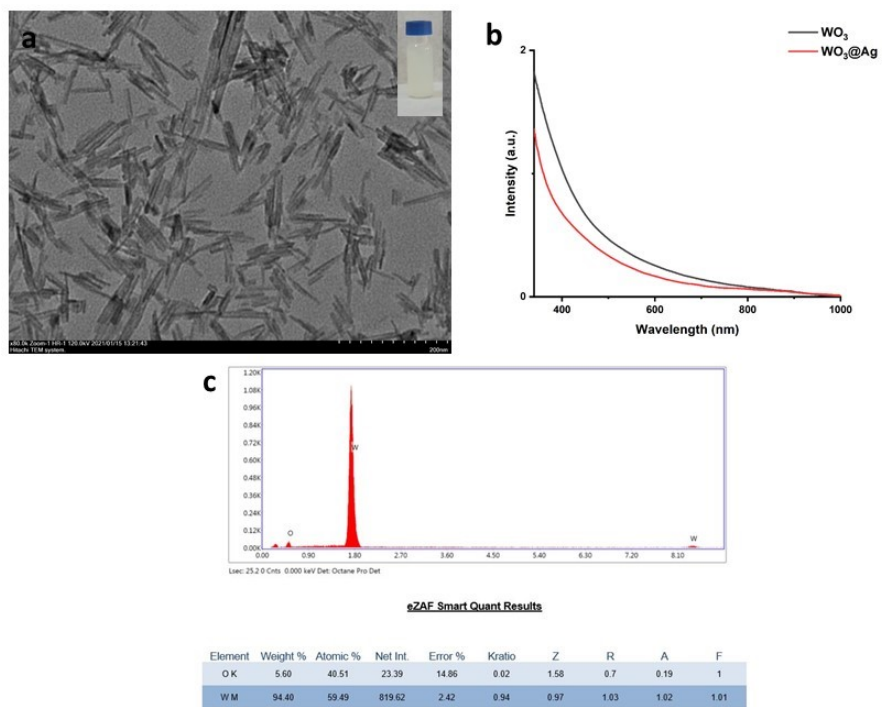


Figure S3. TEM (a), UV-vis absorption (b), and EDX spectra (c) of WO_3 NWs after the addition of Ag ions.

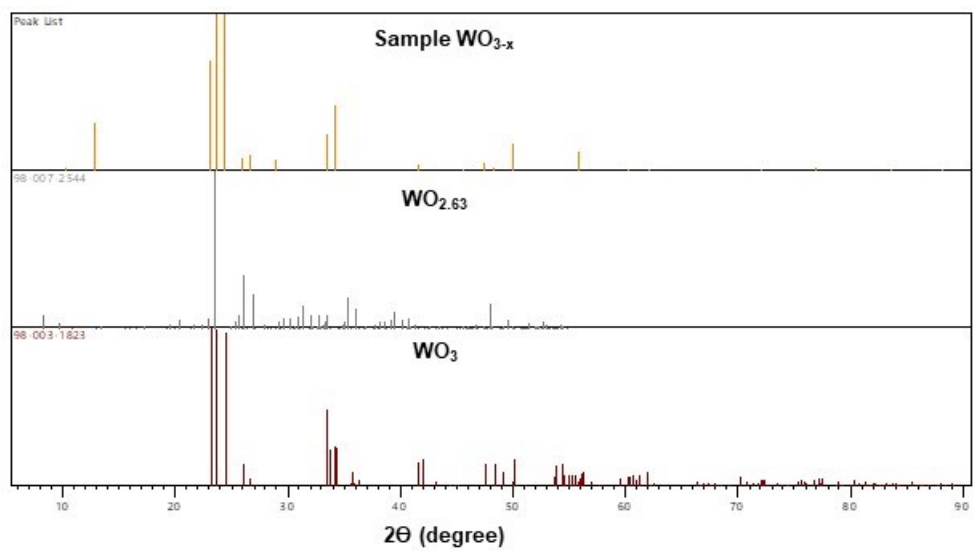


Figure S4. The Rietveld refinement analysis for WO_{3-x} nanosystem.

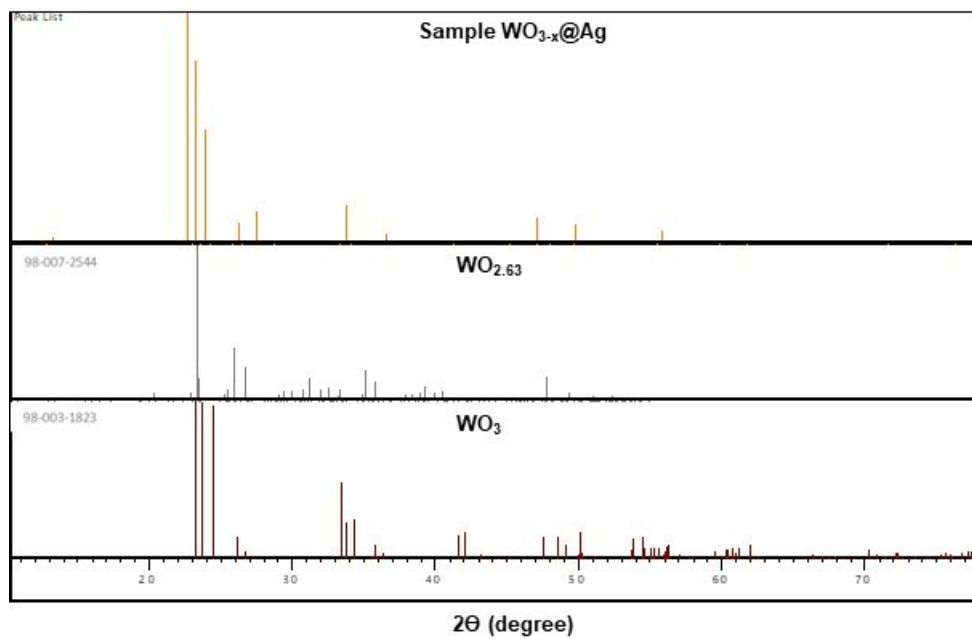


Figure S5. The Rietveld refinement analysis for $\text{WO}_{3-x}@Ag$ nanosystem.

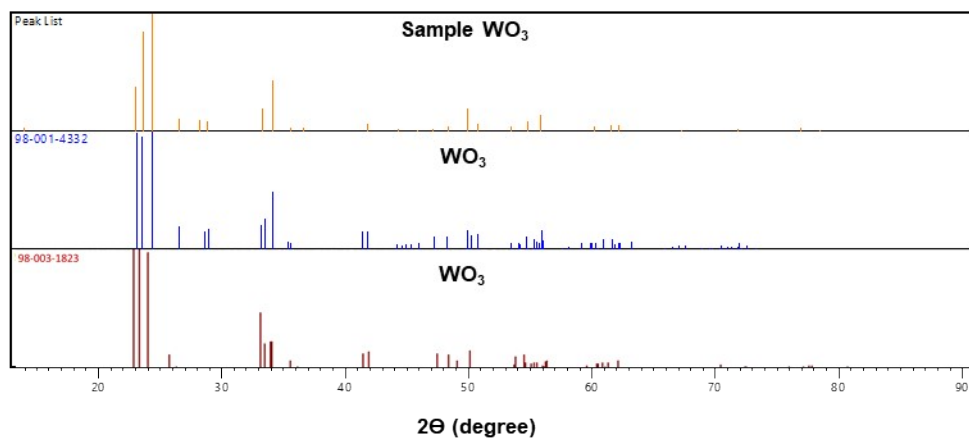


Figure S6. The Rietveld refinement analysis for WO_3 nanosystem.

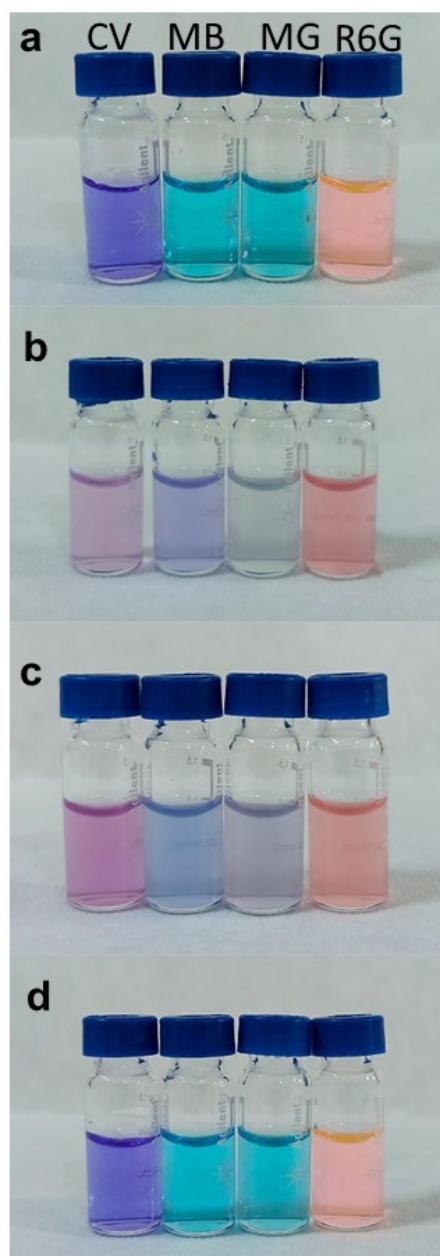


Figure S7. The optic images of pure aqueous dye solutions (a), mixed with WO_{3-x} (b), $WO_{3-x}@Ag$ (c), and WO_3 (d) NP systems. The images were collected immediately after mixing of dyes and NP systems. The final concentration of the dye is 10^{-5} M.

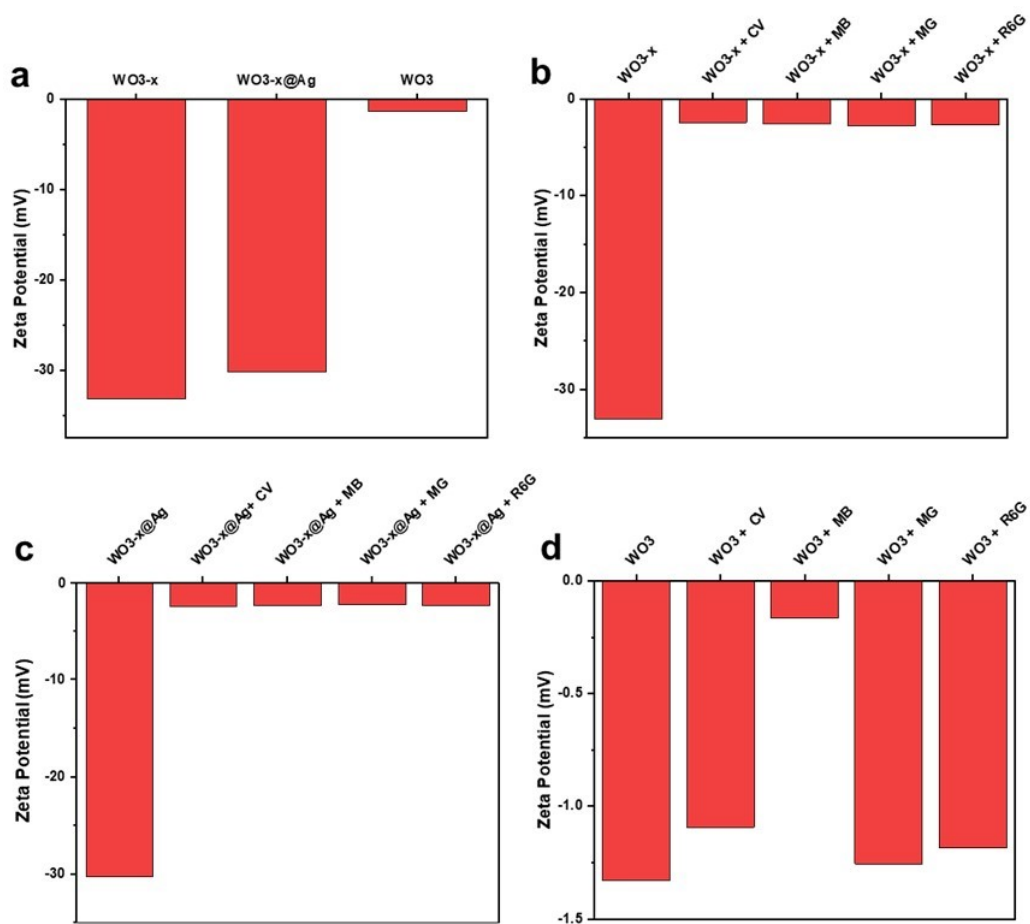


Figure S8. The zeta potentials of pristine aqueous suspensions of NP systems (a) and their mixture with various dyes for WO_{3-x} (b), WO_{3-x}@Ag (c), and WO₃ (d). The final concentration of the dye is 10⁻⁵ M.

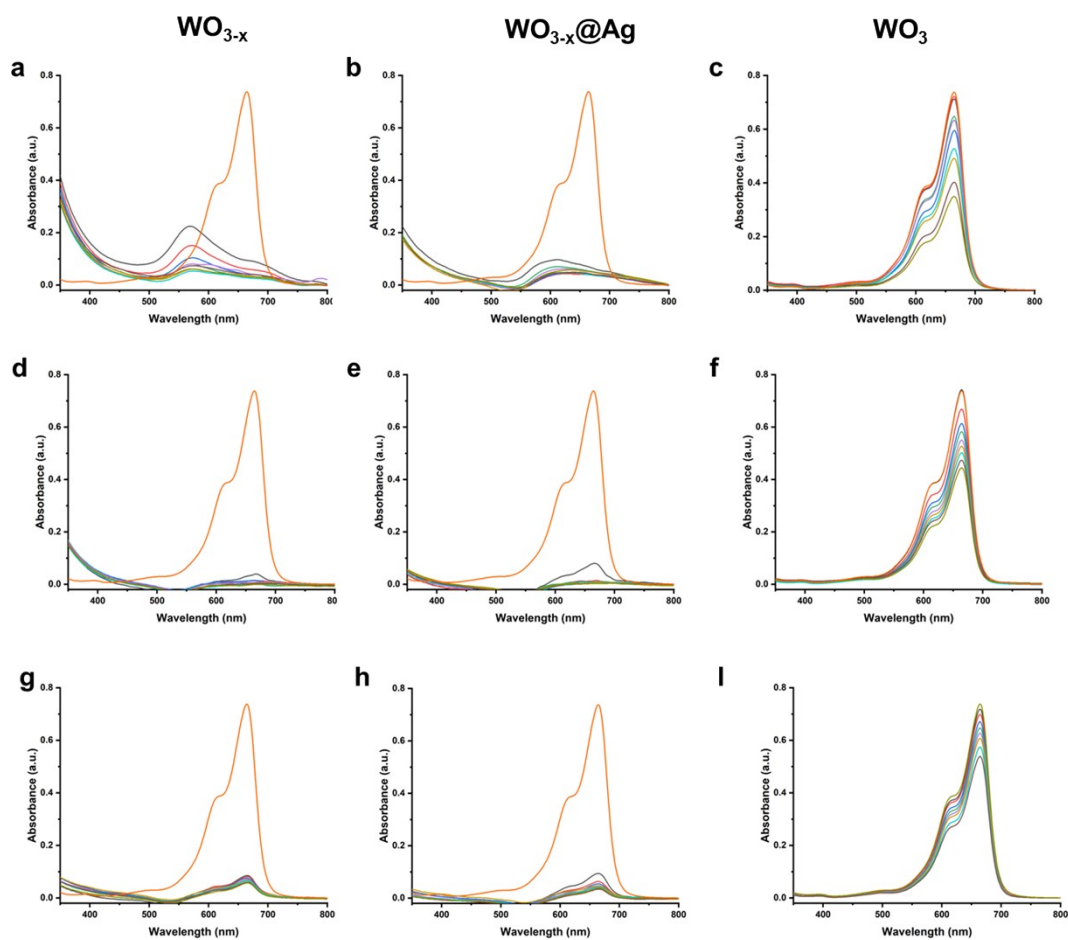


Figure S9. Reusability test of the MB in the presence of different nanosystems. The photocatalytic test was evaluated 3 times for each nanosystem. First cycle (a, b, and c), second cycle (d, e, and f), and third cycle (g, h, and i).

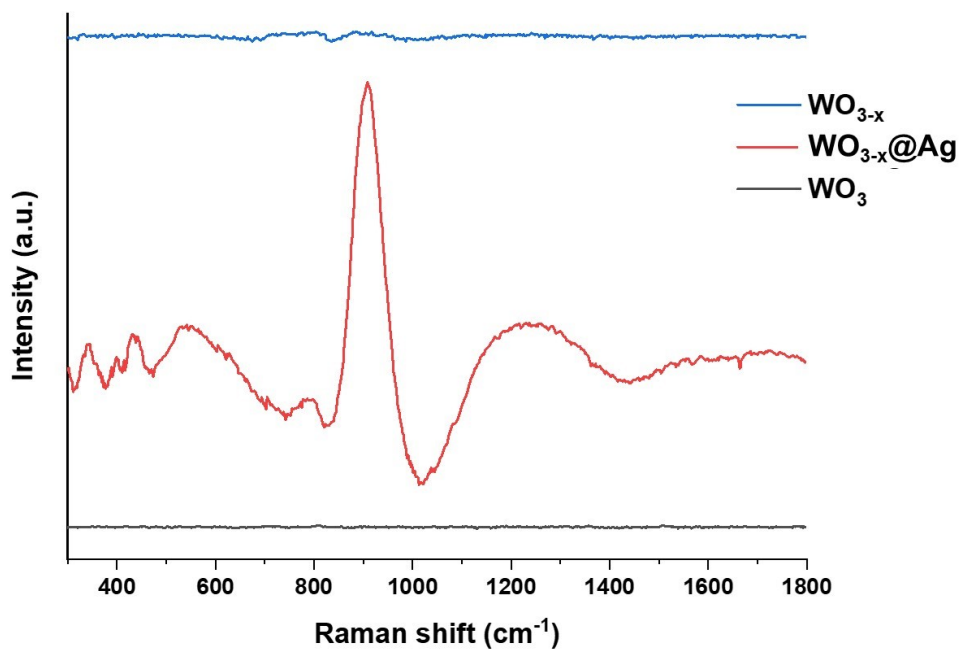


Figure S10. The representative Raman spectra for WO_{3-x}, WO_{3-x}@Ag, and WO₃ NP systems.

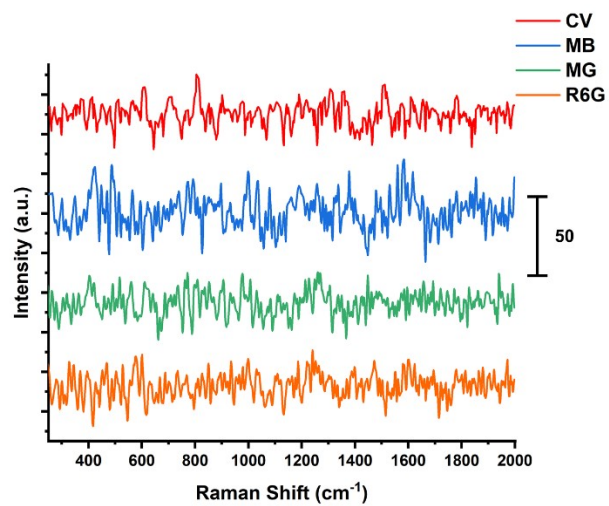


Figure S11. Raman spectra of pure CV, MB, MG, and R6G at 10^{-5} M concentration on aluminum foil without WO_3 -based material.

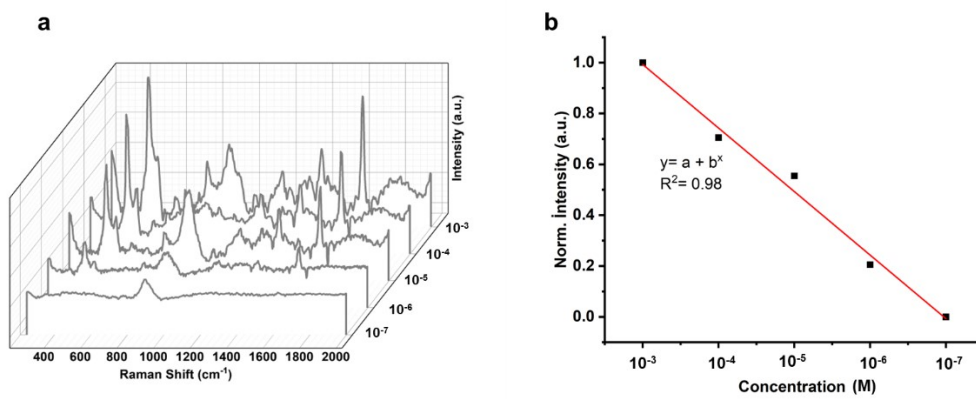


Figure S12. Representative Raman spectra of MB at various concentrations in the presence of $\text{WO}_{3-x}@\text{Ag}$ NP system (a) and normalized peak intensities at 1619 cm^{-1} (b).